Fig. 1

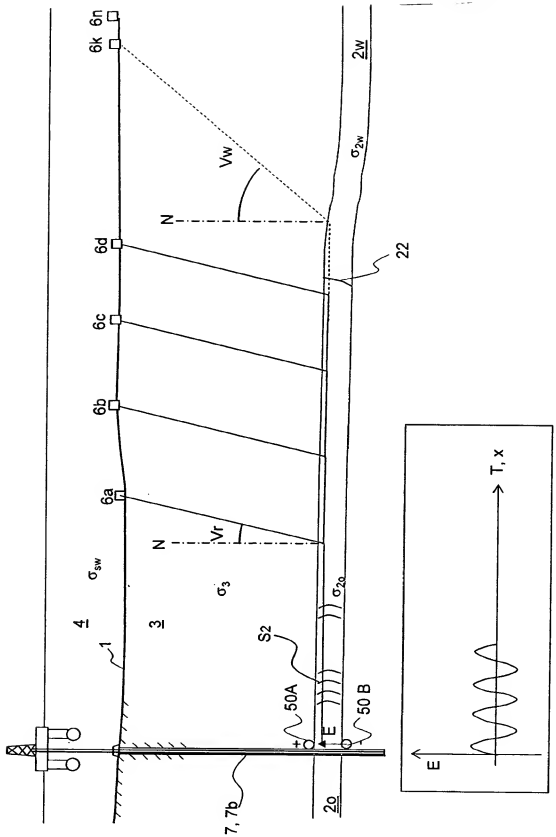

APPROVED: /JMP/

Fig. 2

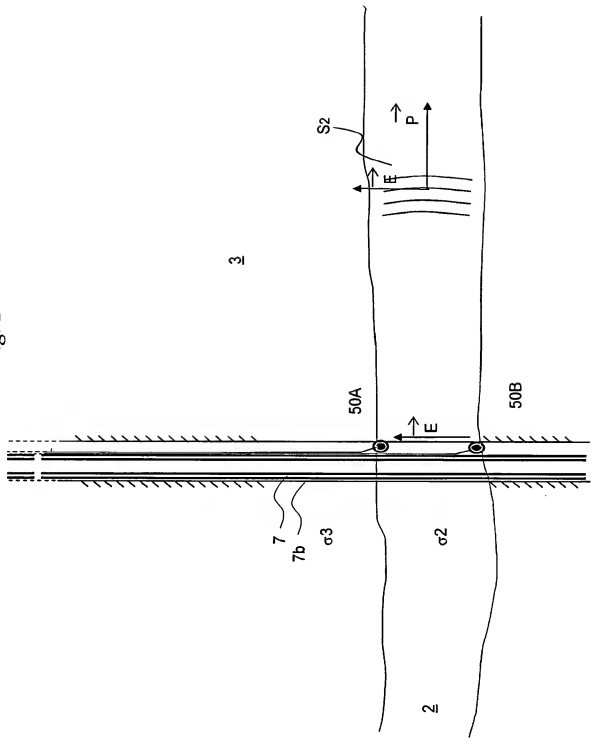

APPROVED: /JMP/

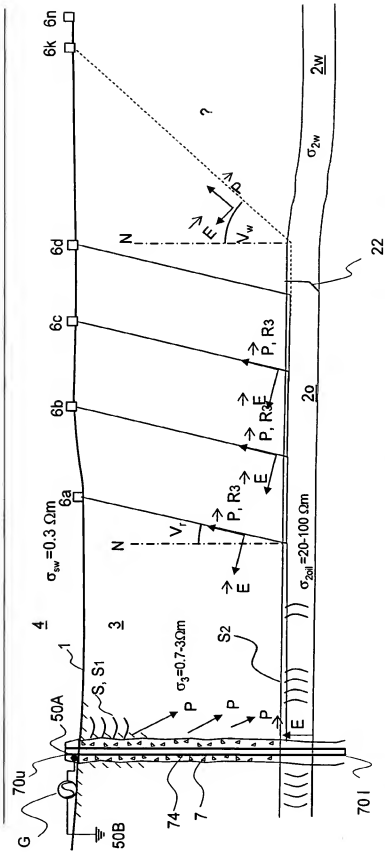
6n
6k
6d
6c
6b
6a
N
V_w
V_r
σ_{sw}=0.3 Ωm
σ_{2w}
2w
σ_{2oil}=20-100 Ωm
2o
22
P, R3
E
4
3
1
S, S1
S2
σ_3=0.7-3Ωm
50A
70u
G
50B
74
7
70 I
A1 (high resist.)
A2 (low resist.)

Fig. 3a

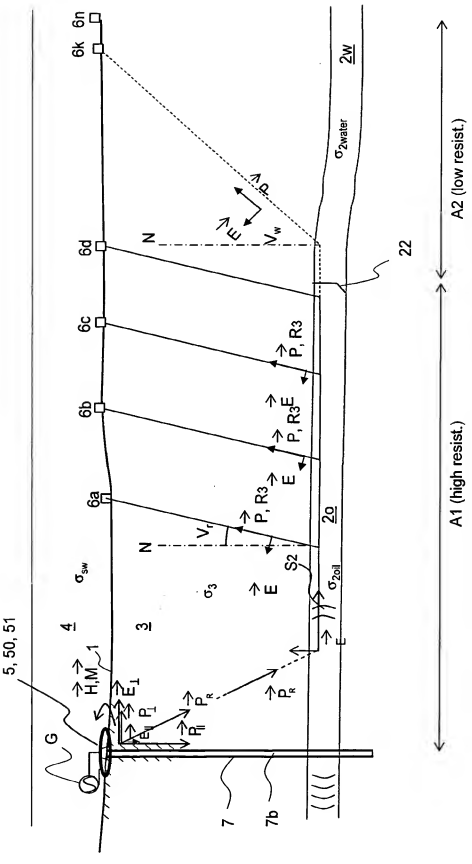

Fig. 3b

APPROVED: /JMP/

Fig. 3c

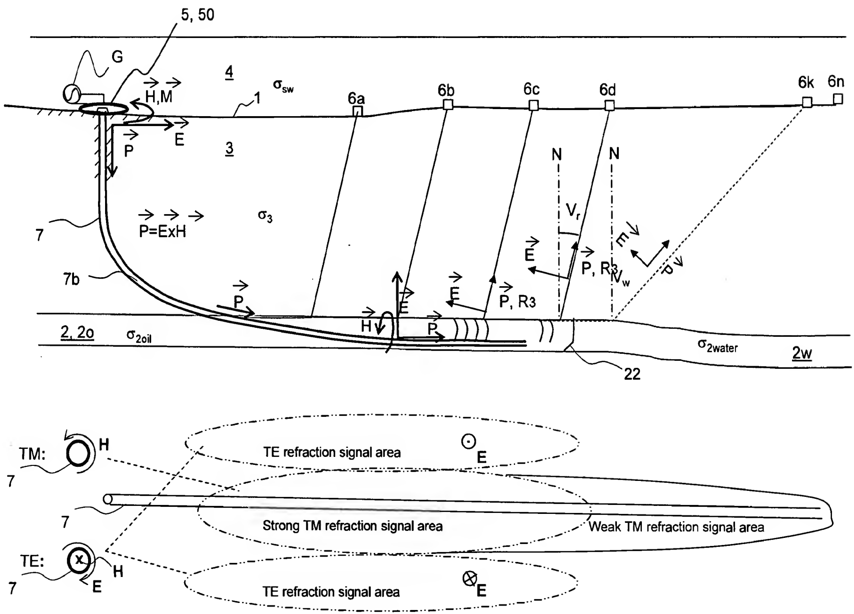

APPROVED: /JMP/

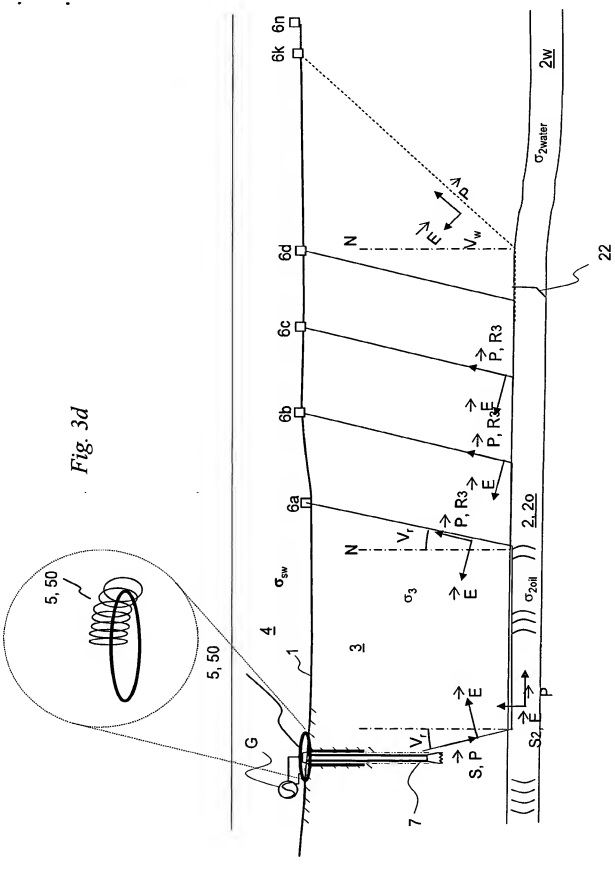

Fig. 3d

APPROVED: /JMP/

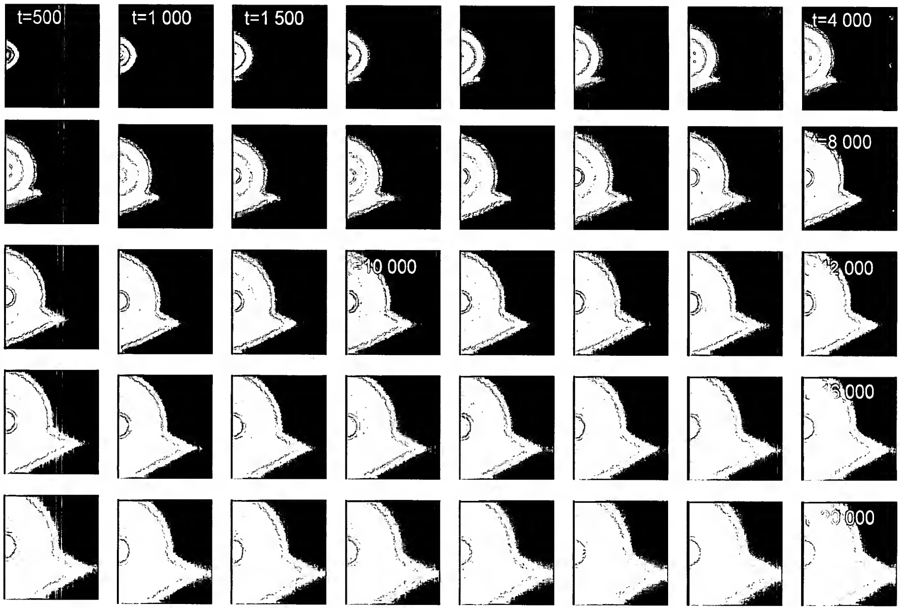

EM wave propagation from 500 to 20000 microseconds.
Time increment 500 microsec,

Fig. 4

APPROVED: /JMP/

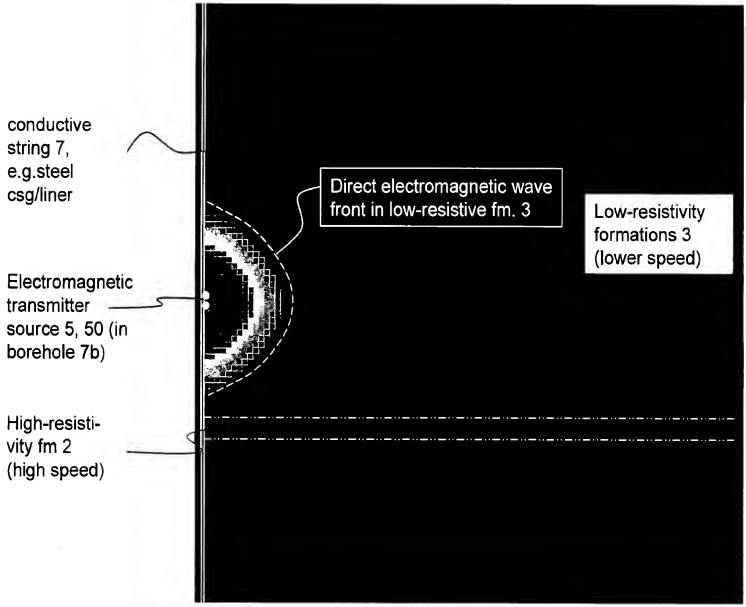

Electromagnetic signal propagated 500 microseconds

Fig. 5

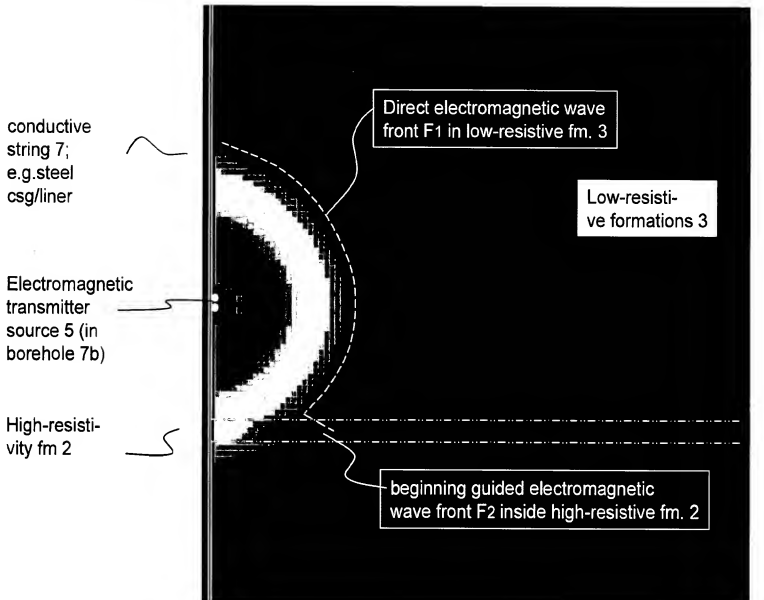

Fig. 6

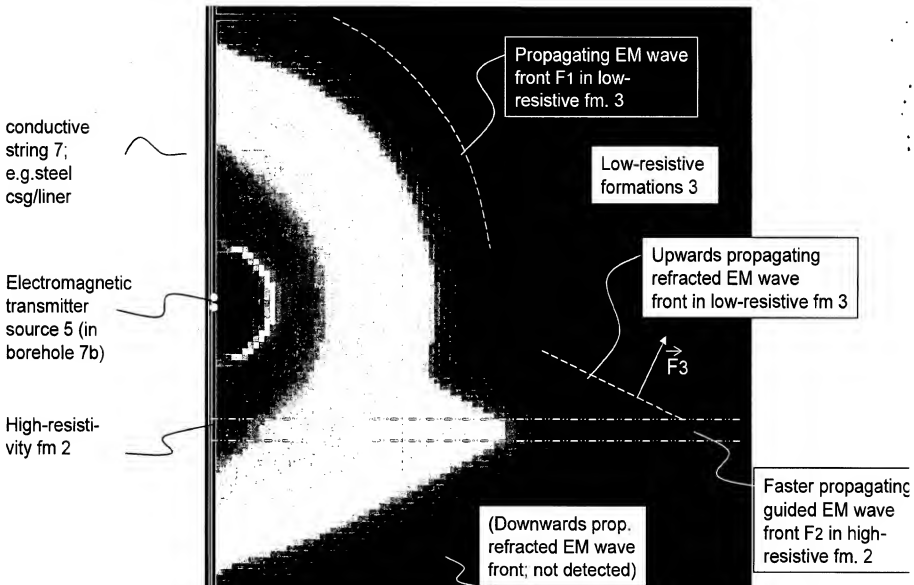

Electromagnetic signal propagated 10 000 microseconds

Fig. 7

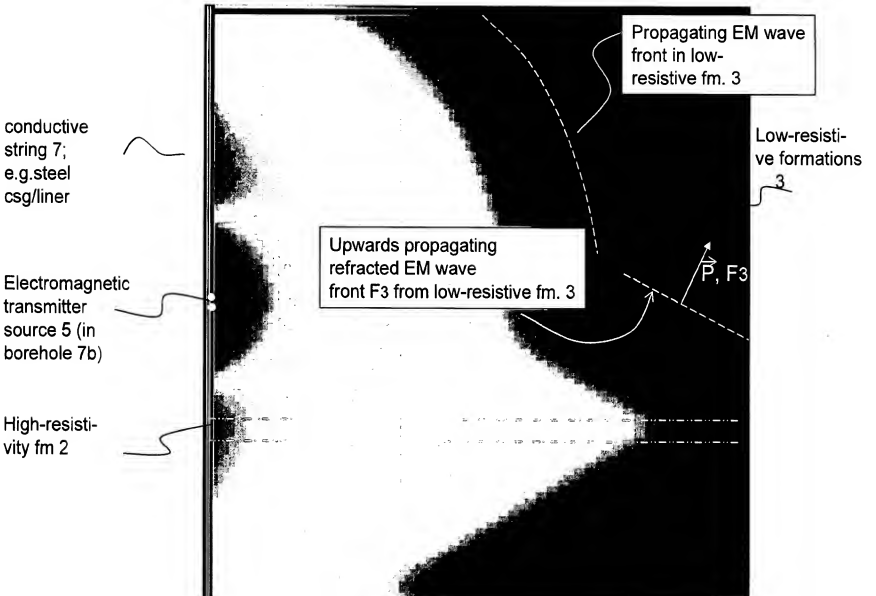

Electromagnetic signal propagated 20 000 microseconds

Fig. 8

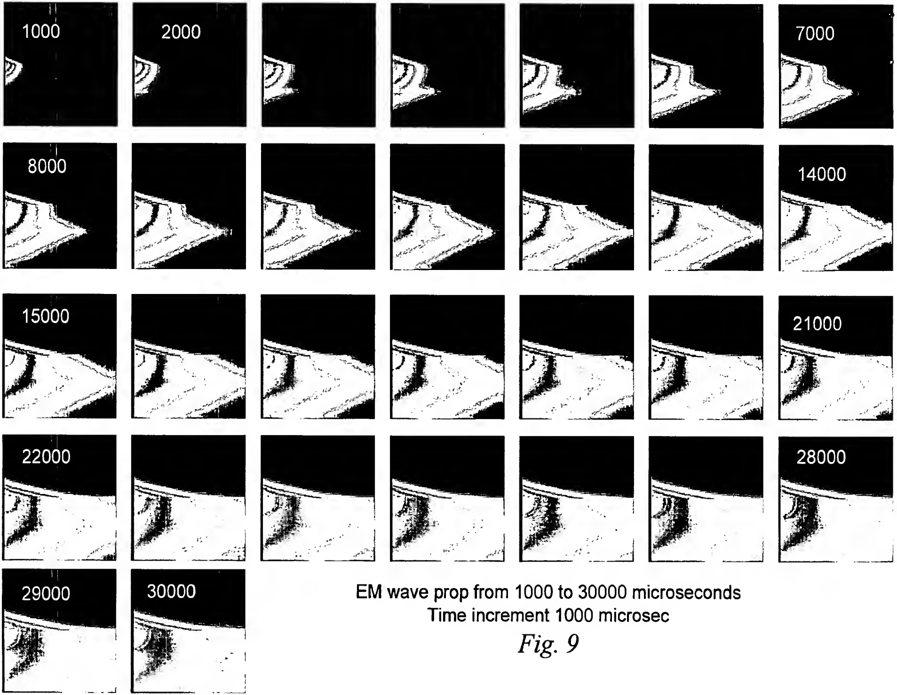

EM wave prop from 1000 to 30000 microseconds
Time increment 1000 microsec

Fig. 9

APPROVED: /JMP/

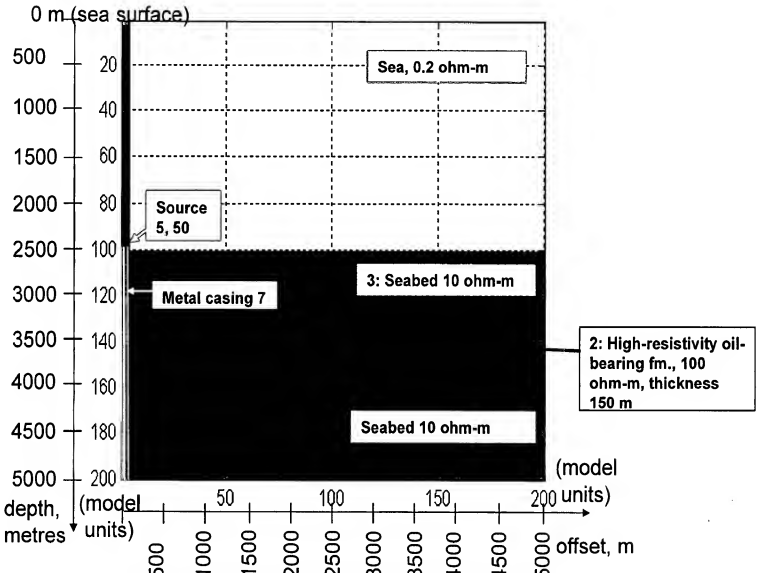

The material model of Fig. 9, indicating a metal casing extending from the seafloor at 2500 m to a total depth of 5000 m into the rocks, with an EM transmitter source on the casing at the seafloor. A high-resistivity oil-bearing rock layer is indicated.

Fig. 9b

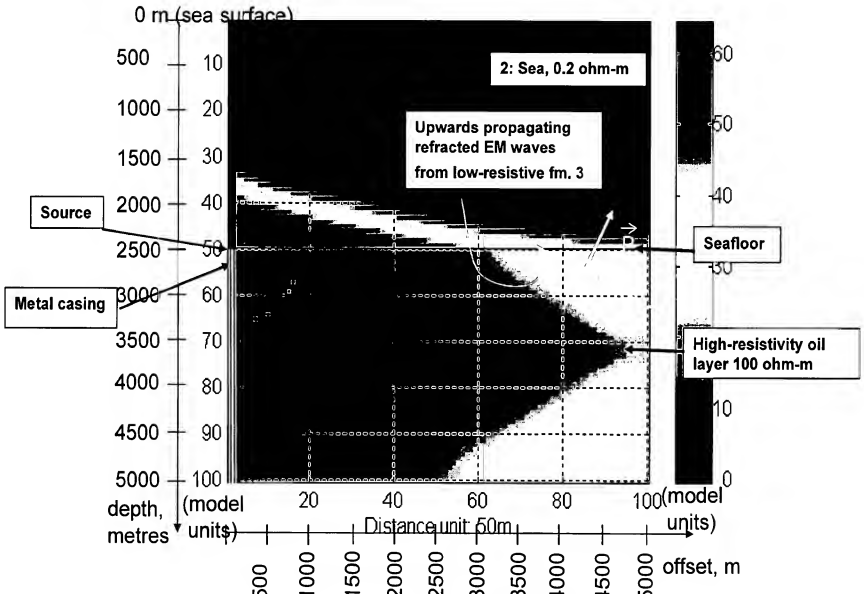

The electromagnetic field intensity according to the model of Fig. 9b.
T= 30 000 microseconds.

Fig. 10

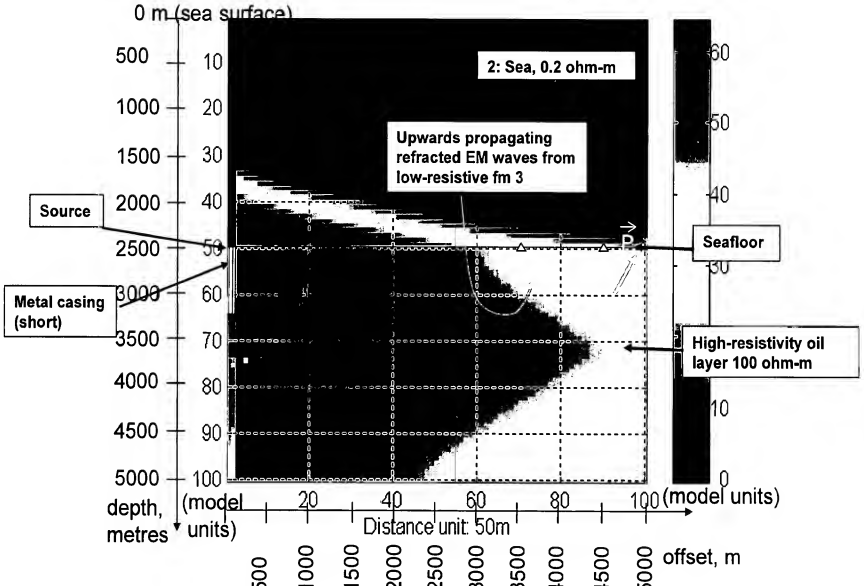

The electromagnetic field intensity according to the model of Fig. 9b, except for a short casing that stops at 3000 m depth below sea surface, or 500 m below seafloor. T= 30 000 microseconds.

Fig. 11

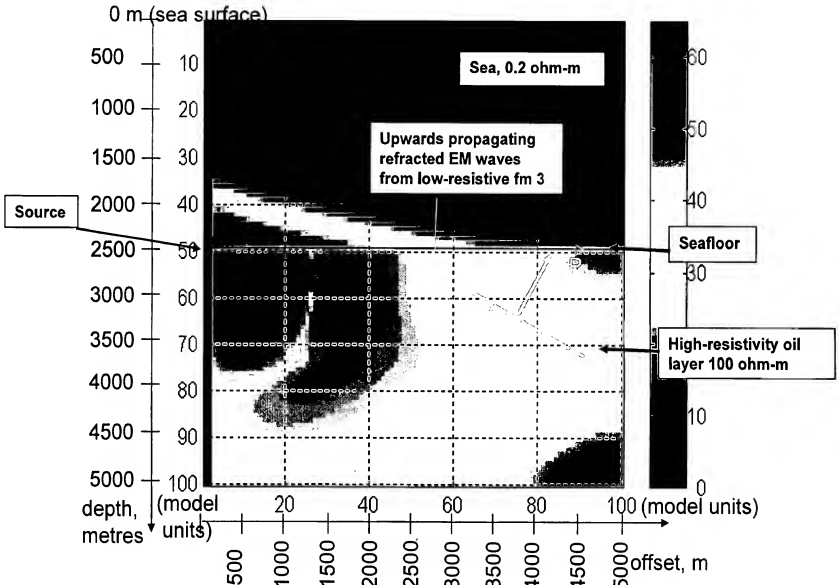

The electromagnetic field intensity according to the model of Fig. 9b, except there being no casing at all in the well. T= 30 000 microseconds.

Fig. 12

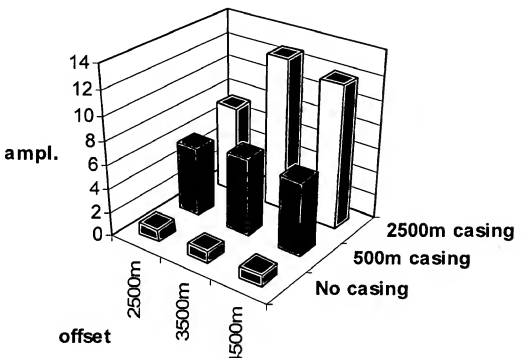

A comparison between amplitudes as measured at the seabed in the imagined situations of having no casing, a short casing and a long casing.

Fig. 13

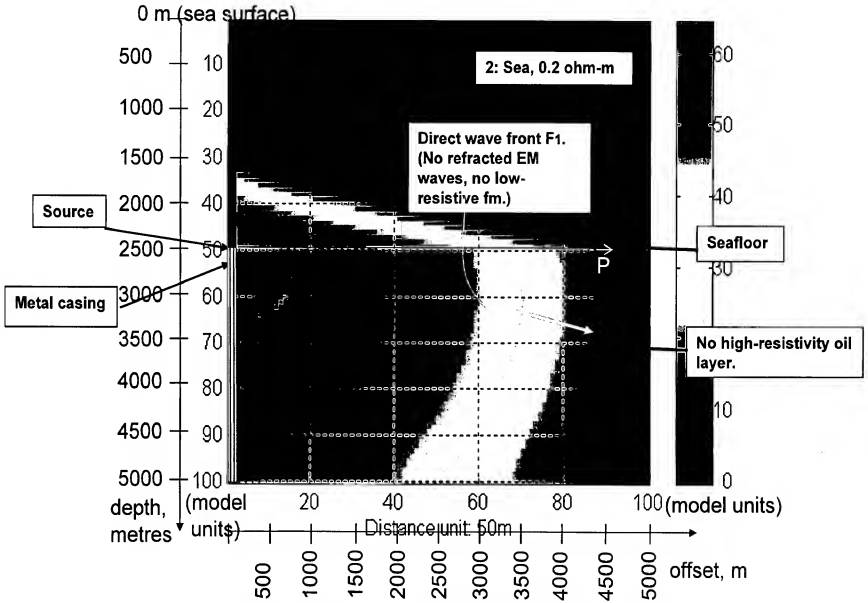

The electromagnetic field intensity according to the model of Fig. 9b, except there being no high resistivity layer.
T= 30 000 microseconds.

Fig. 14